applied sciences

MDPI

Article

Design and Experiments of a Compact Self-Assembling Mobile Modular Robot with Joint Actuation and Onboard Visual-Based Perception

Haiyuan Li [1,*], Haoyu Wang [1], Linlin Cui [1], Jiake Li [2,*], Qi Wei [2] and Jiqiang Xia [3]

[1] School of Automation, Beijing University of Posts and Telecommunications, Beijing 100876, China; wanghy0014@bupt.edu.cn (H.W.); bupt-cll@bupt.edu.cn (L.C.)
[2] X Lab, The Second Academy of CASIC, Beijing 100854, China; phoebeweiqi@hotmail.com
[3] School of Mechanical Engineering and Automation, Beihang University, Beijing 100191, China; xiajiqiang@buaa.edu.cn
* Correspondence: lihaiyuan@bupt.edu.cn (H.L.); lijiake1223@163.com (J.L.)

Abstract: Modular robots have the advantage of self-assembling into a large and complex structure to travel through territories beyond an individual robot's capacity. A swarm of mobile robots is combined through mechanical interconnection and joint actuation to achieve a linked or articular configuration. In this paper, to enhance the perception, actuation and docking capacity of modular robots, a parallel mechanism-based docking system and onboard visual perception system are proposed in the design of a novel compact self-assembling mobile modular robot (SMMRob). Each module is self-contained, with a sensing or joint function. The robot modules can dock with each other based on relative positioning, which employs the visual perception of passive markers or active infrared signals in different localizations. Performance experiments were conducted to evaluate the robot module. Docking experiments were performed, along with an analysis of the success and failure results. The self-assembly of snake-like and quadruped robots was achieved in response to different environments, including an obstacle, gap or stair, and experiments were performed on self-assembly into a snake-like structure.

Keywords: self-assembling robot; modular robot; multi-robot; swarm robot; robot docking; autonomous docking; self-reconfigurable modular robots

Citation: Li, H.; Wang, H.; Cui, L.; Li, J.; Wei, Q.; Xia, J. Design and Experiments of a Compact Self-Assembling Mobile Modular Robot with Joint Actuation and Onboard Visual-Based Perception. *Appl. Sci.* **2022**, *12*, 3050. https://doi.org/10.3390/app12063050

Academic Editor: Oscar Reinoso García

Received: 18 February 2022
Accepted: 14 March 2022
Published: 16 March 2022

1. Introduction

Self-assembling modular robot systems are composed of robotic modules which operate in a swarm fashion and which can dock with each other to collectively form a composite entity with different capacities to respond to environments or tasks. In biology, swarm creatures can move in a coordinated way. Some animals can collectively build massive structures or transporting objects [1]. Although an ant is small, army ants can physically connect together into a bridge to facilitate their travel on curving roads and even dynamically adjust living bridges in response to a cost–benefit trade-off [2]. Self-assembling, self-reconfiguration, self-folding, and self-repair are important ways to change or reconfigure system structures [3]. The architecture of these modular robots can take the form of a lattice, chain, mobile, or hybrid structure.

In the lattice architecture of self-reconfigurable robot system, the modules usually remain connected to structures when the modules perform the self-configuration operation. External help is necessary for the swarm to form a connected structure to build the initial configuration. One motion mode is lattice-based motion, in which the motion space is discrete. MetaMorphic [4], Catoms [5], Kubits [6], and M-BLOCK [7] are able to use revolute motion, prismatic motion, or flying wheels to achieve self-reconfiguration. Modular robots use their self-reconfigurable capacity to change their structure to adapt to environments

and tasks. Lattice modules can be simple to reconfigure for the formation of a complex system but are usually distributed and arranged in discrete locations such as a regular grid.

In a chain architecture, the multiple degrees-of-freedom (DoFs) of joints are used to actuate changes in the structure. CKBot [8], YaMoR [9], M-TRAN [10], and Roombot [11] use joints to reconfigure into a proper configuration which can move in different terrains or manipulate different objects. Although a chain architecture can lift planar structures into articular forms for versatile locomotion and manipulation and offer a tree-like topology, in the self-reconfiguration process, all the modules need to remain connected, resulting in the need for high-dimensional computations.

The initial structure in the lattice or chain architecture is usually built with external assistance, e.g., assembled manually. However, this is unavailable in unstable and hostile environment that humans cannot reach, such as in planet exploration. If the individual modular robots could maneuver appropriately, an initial structure would be formed or disconnected parts could be connected on their own. Therefore, swarm techniques have been combinedinto cooperative multi-agent systems and further self-reconfiguration can be achieved via self-assembly with mechanical interconnection. The S-bot is a mobile robot, with sensors and mechanical connections [12], which can form different connected structures, traversing different terrains and engaging in cooperative transport [13]. Using infrared sensors(IR) and local communication, based on planar self-assembly strategies, mobile robots can dock with each other to build a given structure [14]. E-puck is equipped with a connection mechanism and an external visual position system, and it can complete self-assembling and self-reconfiguring maneuvers through local behaviors. M3Express can move independently and use three dual-purpose wheels, which serve as driving wheels and mechanical inter-connectors to build complex systems [15]. HEX-DMR II employs homogeneous modules and docking mechanisms for self-assembly that can be used to replace individual modules to alter its practical capabilities or replace damaged modules for self-repair [16]. In these mobile robots, joint actuation, mechanical connection and perception abilities are important for docking and self-assembly.

Although an individual may be small or simple, when these individuals are aggregated into a system, these high-level structures become qualified for more tasks. A thousand small swarm robots can cooperate through local interactions in a collective way to form different shapes [17]. Tribot is a small-scale robot with a simple design but it operates collectively to manipulate large objects and overcome obstacles [18]. Without central control, a practical robot system employs a loosely coupled mechanism and stochastic low-level components to achieve robust high-level behaviors [19]. A swarm of identical low-cost quadruped robots were combined with a magnetic docking mechanism and used self-assembly to link to each other in a chain, responding to challenging for individuals such as obstacle navigation and object transporting [20]. SMORES-EP modular robots have been combined with visual sensors to enhance their perception capacity and high-level planning, and local docking and motion were integrated to reactively reconfigure the robot to adapt to different environment types [21]. Swarm robots with mechanical interconnections have another advantage of combiningtools created by humans and bio-inspired schemes. Combining wheeled mobile units and joints in a chain, snake robots consisting of reconfigurable segments can traverse diverse environments [22]. In addition to robots on the ground, a number of self-assembling surface robots [23,24] and aerial robots [25,26] with interconnection capabilities have been proposed.

In a previous work, a modular robot system [27] was proposed to build a variety of bionic structures and an experimental demonstration [28] was performed. According to the docking method, a self-assembly planning algorithm based on local behaviors was presented [29]. However, the mechatronic design can be furtherly optimized for a compact structure such as a snake-like configuration and mobility can be extended to fit more kinds of terrain. In addition, the perception in that case was poor, using only infrared sensors, and joint actuation was insufficient for the assembled structure to attain multiple DoFs of locomotion. In this study, we aimed to propose a novel self-assembling mobile modular

robot (SMMRob) which has better joint actuation with long links and rich visual perception capacities, as well as a well-implemented system. The potential applications include planet exploration, disaster rescue, or field exploration. In these extreme and hostile environments, modular robots can operate in a swarm fashion for wide-area coverage and connect into a multi-joint robotic structure with better terrain adaptability to travel through territories, or a swarm of modular robots can dock with a body platform equipped with a communication radar or solar array in order to advance. The main contributions of our work are as follows.

- A novel parallel mechanism-based joint actuation and onboard vision-based perception system are presented to enhance docking, self-assembly, and actuation for the joints' DoFs. The parallel mechanism can make the robot thinner and enlarge the workspace by longer providing links, which is different from revolute actuators. Onboard vision-based perception improves sensing information and enables the robot to sense autonomously, rather than using external cameras.
- The docking methods for a multi-stage docking procedure based on relative positioning in different ranges are proposed for self-assembly.
- A compact modular robot is designed to make the robot system robust and capable, taking a track-based chassis, as well as mechanically connecting, sensing, actuating and computing performance, into consideration. The modular robot is capable of traveling over different surfaces and the assembled composite entity uses chained wheels and joints to overcome obstacles. Experimental evaluations on module performance, self-assembly, and overall locomotion were performed, showing that the design was implemented well.

2. Design

In this section, the design of a self-assembling mobile modular robot is presented. A modular robot can move on its own but it cannot travel through rough terrain in cases where there are obstacles of a certain height, gaps, stairs, etc., as shown in Figure 1. The aim of modular robots is to enable a group of robots to connect together to create an integrated system that moves, driven either by the wheels of individual modules or acting by means of joints. These robots can collectively move on wheels or lift themselves by means of their linked joints. To enhance the systematic actuation, movement, and sensing capacity, the mechanical and electronic features of the modules are designed herein.

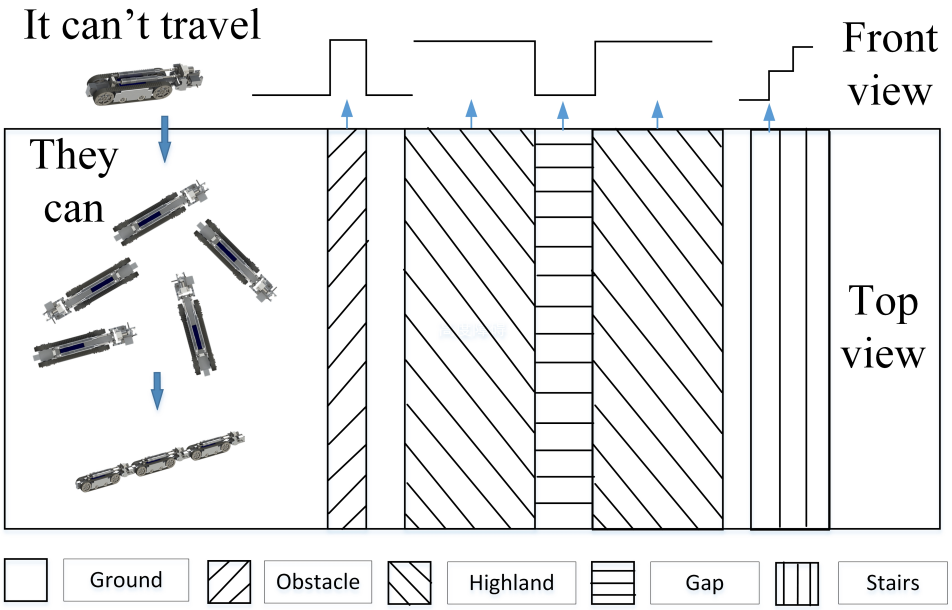

Figure 1. Limited capacity of individual robots and enhanced capacity of self-assembling mobile modular robots by mechanically connecting their modules together. In the front view, it can be seen that there are different terrains such as the ground, obstacles, highland, gaps, and stairs blocking single modular robots, whereas these modular robots can assemble into an articular structure to overcome these difficulties, as shown in the top view.

2.1. Overview of SMMRob System and Module

The integrated modular robot system, the SMMRob system, can have a tree-like topology. Most of this system consists of repeated homogeneous robotic modules, called SMMRob modules. Each module has one active docking panel and/or one or multiple passive docking panels. An SMMRob module can use its active docking panel to connect with the passive one of another module. Each module is self-contained. One of the most commonly used modules is the motion module, used as a composite robot joint body, but to increase their variety, other modules may have additional functions, such as having more cameras, lidars, batteries, or more docking panels, e.g., SMMRob sensing modules, power modules, base platforms, etc. The homogeneous SMMRob modules with different payloads can move, sense, manipulate, and dock individually.

Furthermore, in this paper, the main configuration that the robot modules can connect together to form is a tree-like structure with a thin body, and such a structure may make use ofthe modules' caterpillar track or joints, as shown in Figure 2. The motion modules are used to build the body and the sensing modules are used for the head. The SMMRob module (the default module, referring to the motion module) consists of a thin rectangular chassis, a track drive unit, a docking mechanism, and a joint actuation mechanism, as well as electronic hardware for sensing, control, communication and localization, as shown in Figure 3. A docking mechanism is installed on the front face of the chassis and there is a passive face on the back of the base. The docking mechanism enables each robot module to link to the tail of another module.

Figure 2. A self-assembling mobile modular robot system consisting of a group of self-contained robot modules and modules with a different function forming the head. (**a**) Each homogeneous SMMRob module with a different payload can move, sense, manipulate, and dock individually. (**b**) The robot modules can connect together to form a snake-like high-level system that can move on tracks with joints.

The size of each robot module is 296 mm (length) × 68 mm (height) × 60 mm (width). The chassis provides the base for the track drive unit, which is a differentially driven and can move forward and backward and rotate. A drive pulley for each track is driven by a gear-reduced DC motor (DC 7.4V, KingMax, China) with a magnetic encoder. There are two idler pulleys on each side to support the track and adjust the tension. A summary of parameters such as dimensions, weight, actuation strength, etc., are shown in Table 1.

Table 1. A summary table of the parameters of SMMRob modules.

Term	Value
Dimensions	296 × 68 × 60 mm
Weight	900 g
Battery life	120 min (track motion)
Max. linear speed	40 cm/s
Max. payload	8 kg
Communication	ZigBee/WIFI/CAN bus
Sensor	Camera/UWB/IMU/Encoder
Joint torque	2.7 Nm
Range of yaw	−30°∼ +30°
Range of pitch	−45°∼ +45°

The sensing module at the head of the snake-likesystem is equipped with a laser distance sensor (TFmini-S, operating range: 0.1–12 m, Benewake, China), a stereo camera, and a wireless video transmitter. The lidar can measure the distance of the target in front and can even be combined with a pitch and yaw joint to build a sparse point-cloud model of the environment. The stereo camera, providing video with 720P resolution and at 30

frames per second, can be used for detection and the operator can receive the remote-field video in real-time.

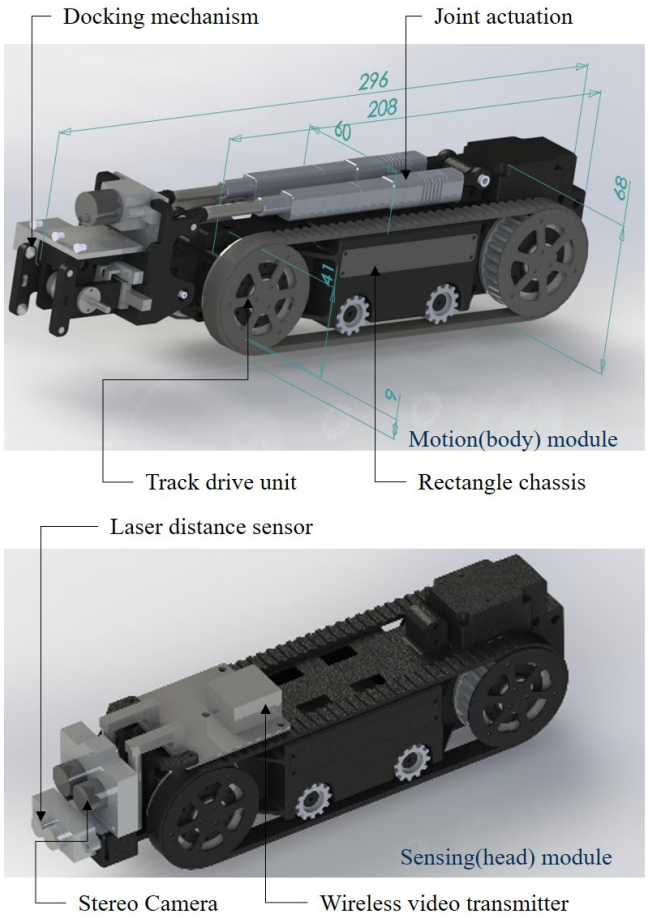

Figure 3. The overall design of SMMRob modules, including the motion module (default) and sensing module. In the self-assembled snake-like system, the motion module is a component of the body, whereas the sensing module is used as the head. The unit of length is mm.

2.2. Docking Mechanism

The principle of the docking mechanism is based on a parallel gripper that can connect or separate two parts, e.g., two robot modules or a robot module and a station. The docking mechanism consists of two separate parts, an active part at the front of one robot module and a passive part at the back of another robot module, as shown in Figure 4. In the middle of a passive part, there is a rectangular solid, where two conoid grooves on each side are designed, and there are two corresponding conoid pins on each side of the active part. When docking, the conoid pins are inserted into the grooves. Even if the pin and groove are not aligned, within an expected certain displacement distance ($d < 2$ mm, as shown in Figure 4b) and displacement orientation ($a < 6°$) in Figure 4c, the conoid form can guide the two parts to completely match. The passive system can work without power.

As shown in Figure 4a, the active part can drive two opposing jaws (XI) to travel in parallel to make the pin (XIII), which is inserted into or pulled out of the grooves (IV). The closing and opening of the jaws are achieved by means of a pair of bidirectional lead screws (X) and nuts (IX). The two opposite sections of the lead screw are left-hand and right-hand thread-mated, respectively, with two lead nuts. The lead nut is installed into a sleeve inside the connecting structure, rigidly connected to a sliding block (VIII), resulting in limiting the rotation but allowing the axial movement of the nut. Meanwhile, the upper and lower sliding blocks on the frame of the active part can support the docking mechanism for a large payload. The lead screw is driven by a DC motor via gear transmission. A linear

potentiometer is equipped onto the frame to measure the displacement of the nut to provide feedback of for the opening and closing of the jaws. After docking, the spring contact (XII) of the active part can touch the contact socket of the passive part to achieve CAN bus communication. The lead screw and nuts are self-locking and therefore the docking mechanism will maintain a stable connection and will not unexpectedly separate when the lead screw is at rest with the motor power turned off.

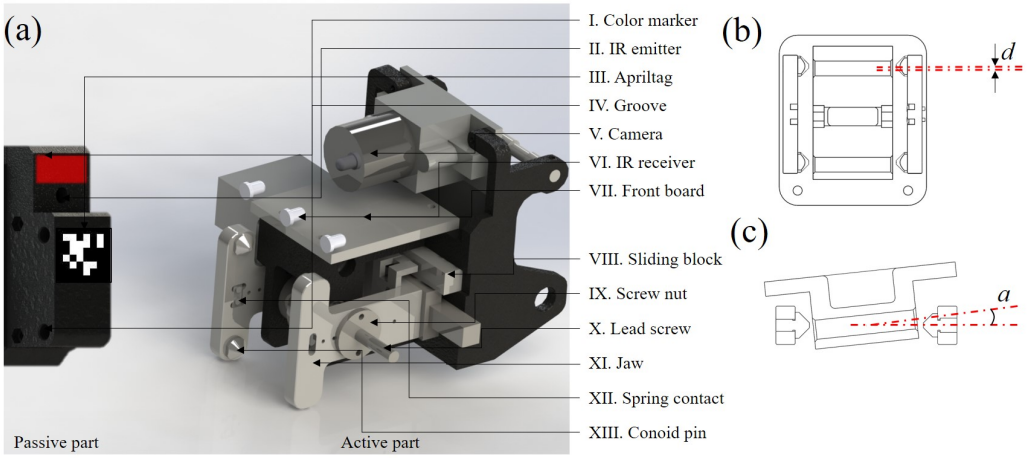

Figure 4. Docking mechanism and sensors for docking. (**a**) The passive part includes the grooves and the electrical contact socket. The color marker and Apriltag marker are used to indicate the position and orientation in different distances of the front robot module, as well as robot identifier (ID number). The IR emitter is used with the receiver of the active part to guide nearby docking. The active part integrates a pair of opposing jaws, driven by a bidirectional lead screw and nut mechanism. The camera can recognize the markers and provide the coordinate and ID information. (**b**) Displacement distance d between the pin and groove axis from the front view. (**c**) Angular displacement a between the pin and groove axis from the top view.

2.3. Joint Actuation

With the joints between two connected modules, the composite system can lift itself and move like a snake or legged robot. To enhance the joint actuation, a 2-SPS parallel mechanism was designed to achieve two degrees of freedom in the position of the docking mechanism, as shown in Figure 5. The docking mechanism is connected to the chassis by two orthogonal hinges, which are constrained to yaw and pitch motion with respect to the chassis. Each SPS kinematic chain is driven by a linear actuator (LA series, Beijing Inspire Robots, China) with two non-driven spherical pairs. The yaw motion occurs when the two linear actuators are differentially pushed/pulled and the pitch motion occurs when the actuators are controlled to move away from the initial position. Simultaneous yaw and pitch motion can be achieved by two actuators, using kinematics that are described in Section 3.

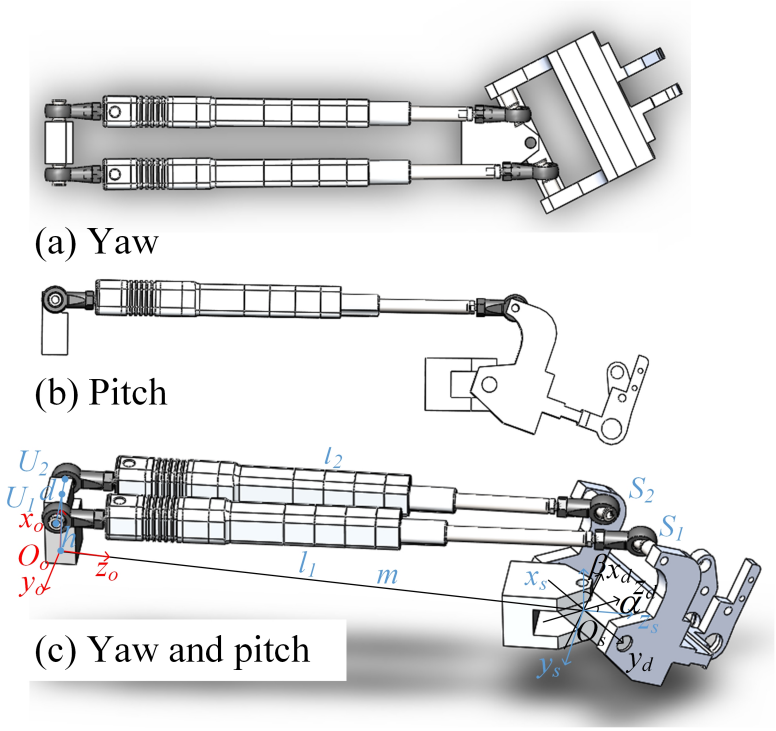

Figure 5. Two degrees of freedom of the 2-SPS parallel mechanism. (**a**) The yaw motion is controlled via differential displacement of the two actuators. (**b**) The pitch motion is controlled via the displacement away from the initial position. (**c**) The orientation is achieved via simultaneous control of the two actuators.

2.4. Sensing, Control, Communication, and Localization

2.4.1. Sensing

In different components, different types of sensors are equipped to measure the relative position and orientation. The camera (image sensor: OV5640) and infrared sensor (940 nm) are used to guide the docking process in different stages. As shown in Figure 4, color markers (red) and Apriltags are used as the passive markers to be recognized by the camera. The color marker can indicate the alignment and distance. The Apriltag can provide the coordinates of the marker in the frame of the camera. An infrared emitter is installed on the passive part of the docking mechanism and three infrared receivers are distributed along the transverse side of the active part of the docking mechanism. According to the infrared signal strength, the robot can measure the distance and alignment in a short range. In addition, an inertial measurement unit (ATK-IMU901, Alientek, China) is integrated inside to provide feedback regarding the attitude in extended functions.

2.4.2. Control

The computing of different algorithms requires the corresponding hardware to balance performance with costs in terms of time and power consumption. A Raspberry main board (1 GHz CPU), acquired off the shelf, is used to run the main software to deal with docking, movement, and coordination tasks. The motor actuation, low-level sensor management, and chassis motion control is dealt with by an ARM-based motion controller board (168 MHz MCU) developed by ourselves. The motor and infrared sensors of the docking mechanism are managed by an ARM-based front board (72 MHz MCU) developed by ourselves. These ARM boards communicate with the main board via USART. The visual recognition using video in the docking system is processed by an ARM-based visual processing board (480 MHz MCU) which communicates with the main board via SPI bus because a high-speed interface is necessary to stream image data. The control hardware system is shown in Figure 6.

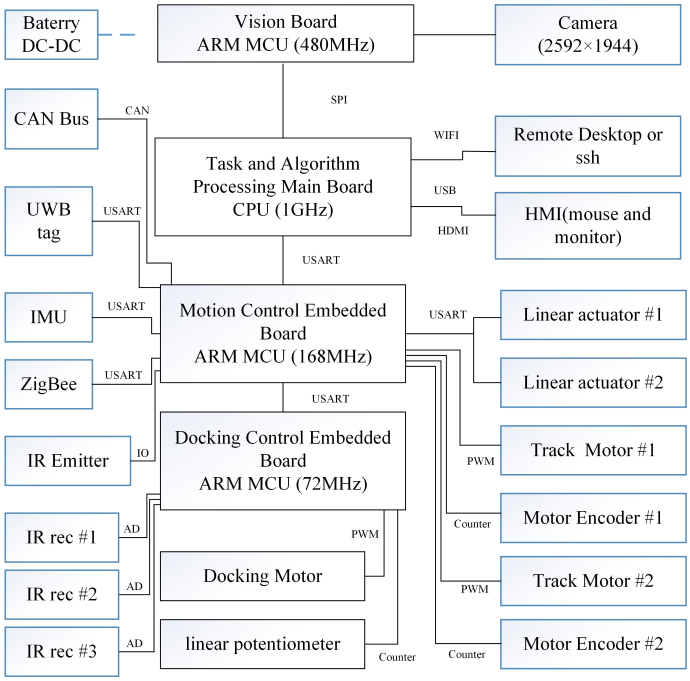

Figure 6. The hardware for sensing, control, communication, and localization, the communications between circuit boards and the main input/output pins.

2.4.3. Communication

A swarm of modular robots can communicate with each other via ZigBee-based wireless sensor networks. Each robot module has a Zigbee board with antennas covered by a plastic shell. In a group of robot modules, the Zigbee device of the head module operates as the coordinator, whereas the other devices of the body modules operate as the end-devices. If there are several groups of swarms, only one head is selected as the coordinator and other head modules are selected as the routers as messengers for communications between other body modules operating as end-devices. The robot can send messages to the target robot with a short address on the same channel. When the robot swarms finish the assembly process, they can communicate using CAN bus. In addition, WiFi is available to all the modules.

2.4.4. Localization

In this study, our aim was to use local sensors to guide the robots to dock with each other without a global/external positioning system. In short ranges (with distance between two robot modules less than 2 m), SMMRob can locate itself using the robots' internal sensors and cameras with respect to other robots (relative positioning will be presented in Section 3.3.1). Initially, these robots will be deployed in short ranges to find other modules using cameras and they can search for others randomly. Meanwhile, to provide a wide-ranging application in future, an ultra-wideband (UWB) positioning system is integrated. Each modular robot is equipped with a UWB terminal chip or called tag, and four positioning anchors distributed in four different positions. UWB can provide sub-meter-level positioning accuracy. The UWB system will be used for further research in the future and is not used in this paper.

2.4.5. Software and Protocol

The main applications run at the main board with a Linux system. The front board and motion controller board deal with the low-level applications, e.g., chassis velocity control, IMU reading, UWB reading, Zigbee data transmission, and docking open/close mechanisms, etc. with non-operating system (OS) firmware and can be called by the main board using the communication protocol. The visual processing board performs different

visual recognition and measurement applications, providing these data to the main board when requested, or it can be set to a timing mode. The protocol defines the frame object, command, and parameters. In addition, the Zigbee board is directly connected to the motion controller board. Therefore, the low-level controller function can be called via remote procedure call (RPC) by another modular robot or an upper-level computer.

3. Control Methods

A group of SMMRobs run in a swarm fashion. Each robot is self-contained and individual. When one of the robots encounters a gap, obstacle, or larger manipulating objects, it is unqualified and cannot overcome it by itself. According to a prior structure library, a proper configuration is selected and described using a tree with nodes representing robots and edges representing docking positions. The tree determines the allocation of roles for each robot in the self-assembly process. According to the self-assembly planning sequence, the individual SMMRob modules dock with each other to form the target structure. Self-assembly can incorporate the low-level SMMRobs to form a high-level system to achieve terrain trafficability, obstacle crossing, stair climbing, or complex object-manipulation tasks that are beyond the performance of the individual modules. The modular body robots are homogeneous and dock with each other in tree-like configuration such as a snake or a quadruped configuration. After self-assembly, the tracked snake-like robot can move on wheels or operate using joints. The control scheme of self-assembly for a swarm of SMMRob robots into a target structure is shown in Figure 7. The self-assembly configuration planning, model, and docking control method of each SMMRob are presented in this section.

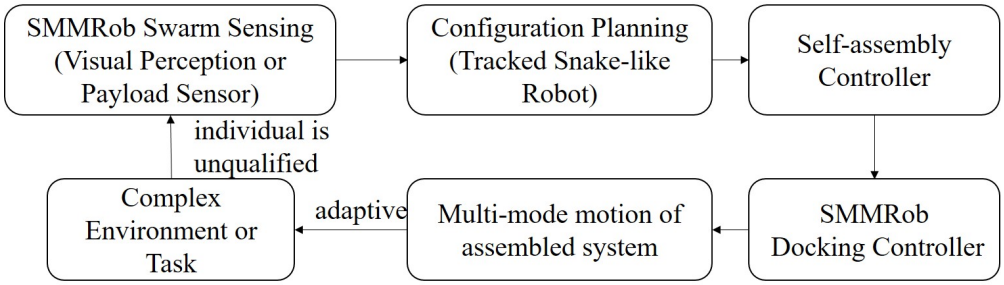

Figure 7. Overview of the control flowchart.

3.1. Self-Assembly Configuration Planning Sequence

Each modular robot may have an active docking panel on its front (numbered 1) and four passive docking panels on both lateral sides (numbered 2, 3, 4, and 5, respectively) with one passive docking panel in the rear (numbered 6) as shown in Figure 8a. Given the topology of the target structure, in which a node presents the robot number and an edge indicates the passive panel number in the parent node (see three examples of a snake-like, quadruped, and quadruped structure with a spine in Figure 8b,c) and each node can be visited based on a breadth-first search algorithm. According to the breadth-first visit sequence, the robots at the same level can dock with the parent node simultaneously, e.g., in Figure 8d, robots 2, 3, 4, 5, 6 SMMRob can dock with robot 1 at the same time, whereas SMMRob robot 3 has to wait to dock until robot 2 finishes docking.

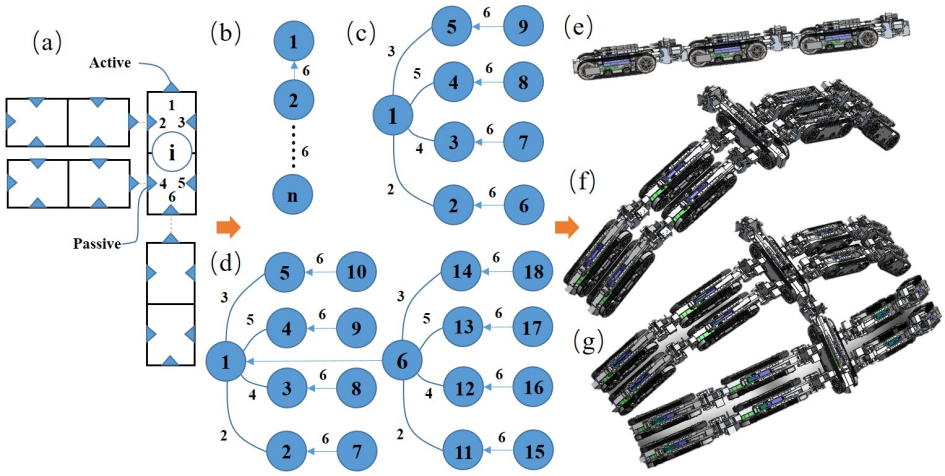

Figure 8. SMMRob topology and diversity of structures. (**a**) Allowed active and passive docking panels. (**b**) Linear configuration topology. (**c**) Quadruped configuration topology. (**d**) Quadruped configuration topology with a spine. (**e**) Snake-like structure. (**f**) Quadruped structure. (**g**) Quadruped structure with a spine.

3.2. Model of SMMRob

3.2.1. Mobile Kinematics

An SMMRob moves on a caterpillar track and is differentially driven. Taking no consideration of sliding and assuming the fixed instantaneous centers of rotation of treads, the kinematics of this robot can be modeled using a differential system, expressed as Equation (1).

$$\begin{cases} v = \frac{R}{2}(\omega_R + \omega_L) \\ \omega = \frac{\omega_R - \omega_L}{n} \end{cases} \tag{1}$$

where v and ω are linear speed and angular speed, respectively. R is the radius of the drive wheels and n is the lateral axis distance of the chassis, whereas ω_R and ω_L are the angular speed of the right and left servos, respectively, which are calculated using encoder pluses. These variables are depicted in Figure 9b.

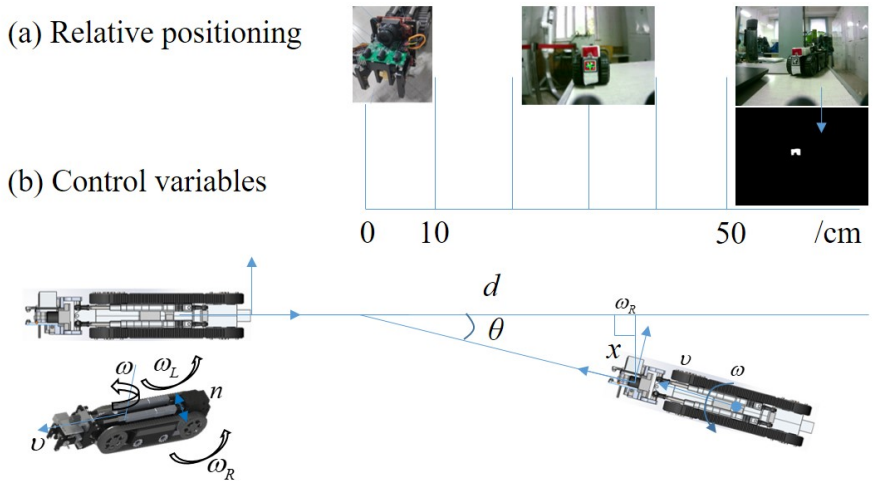

Figure 9. Relative positioning, and controllable and measured space in plane.

3.2.2. Kinematics of Joint Mechanism

The inverse kinematics of the 2-SPS parallel mechanism is used to calculate the displacement of two linear actuators according to give the yaw α and pitch β angles of the

docking mechanism. As shown in Figure 5, a follow-up coordinate O_d is built at the hinge center of the docking mechanism, whereas the coordinate O_s is connected to the chassis, initially aligning with O_d and the chassis and a body coordinate O_o is connected to the chassis, originating at the intersection of the vertical axis and the longitudinal axis. The transformation matrix between O_d and O_o is expressed in Equation (2).

$$T_d^o = T_s^o T_d^s = trans(m, Z_o) rot(\alpha, X_s) rot(\beta, Y_d) \tag{2}$$

where m is the distance between the origin points of O_d and O_s, S_1 and S_2 are the spherical center of 2-SPS on the docking mechanism, and U_1 and U_2 are the spherical center of 2-SPS on the chassis. The coordinate transformation of the point S_i $(i = 1, 2)$ from O_d to O_o can be obtained using Equation (3) when the joint operates.

$$\begin{bmatrix} {}^oP_{S_i} & 1 \end{bmatrix}^T = T_d^o \begin{bmatrix} {}^dP_{S_i} & 1 \end{bmatrix}^T \quad i = 1, 2 \tag{3}$$

The controlled displacement of linear actuators can be calculated using Equation (4).

$$l_i = \sqrt{({}^oP_{S_i} - {}^oP_{U_i})^T ({}^oP_{S_i} - {}^oP_{U_i})} \quad i = 1, 2 \tag{4}$$

3.3. Docking Method

3.3.1. Relative Positioning

The relative positioning method assumes that the later robot module and the front robot are on the same plane without rolling. The aim of docking is to align the later one with the front one and park them at a certain distance away from each other. The measured feedback variables are distances and angles between two robots as defined in Figure 9b.

- x is the lateral distance.
- d is the longitudinal displacement.
- θ is the difference in the heading angle of two robots.

In different distances between two robots, the precision and perception ranges of relative positioning are different.

- In the far range ($d > 50$ cm), the color marker of the passive docking panel is recognized by the camera. It has a wide detection field and an easy-to-process algorithm. The color marker indicates that this may be a robot without an ID. The lightness, green value, and red values in LAB color space are used for target segmentation and the markers' geometric center in pixel units is the target position. The binary image with a white block indicating the color marker is shown in Figure 9a.
- In the middle range (50 cm $\geq d \geq$ 10 cm), the encoded marker (Apriltag) is used to guide docking. The visual processing board can generate the coordinate and bounding-box information (see Figure 9b) of the Apriltag and transfer them to (x, d, θ). Although the recognition range is minimized, the precise coordinate is given and the robot is identified by its ID.
- In the near range ($d < 10$ cm), the color and Apriltag marker pass beyond the field of view of the camera. The infrared sensors are used to guide the robot based on signal strength, expressed as d, and the weighted average of the lateral distances of three infrared receivers, expressed as θ.

3.3.2. Docking Controller

According to the relative positioning, a piecewise controller based on the PID algorithm is proposed to guide docking as in Equation (5). The control inputs v and ω refer to linear velocity and angular velocity, respectively.

$$v, \omega = k_d f_d(d - d^*) + k_x f_x(x - x^*) + k_\theta f_\theta(\theta - \theta^*) \tag{5}$$

The piecewise controller aims to minimize the errors of three variables ($\Delta x = x - x^*, \Delta d = d - d^*, \Delta\theta = \theta - \theta^*$) referring to the target feature values. The control flowchart and switching scheme between different states are shown in Figure 10.

- Image-guided approaching controller. In the far range, the docking controller is based on an image-guided approaching scheme. v and ω are controlled and k_x and k_θ in image coordinates with pixel units are scaled up to minimize Δx and $\Delta\theta$. The PID controller is used, expressed as f. When the size of the color marker is larger than the threshold or the Apriltag or an infrared signal is detected, it switches to the next corresponding subroutine.
- Position-based approaching controller. In the middle range, the coordinates including the position and yaw angle can be calculated in time. k_θ is scaled up to control ω to align the heading and v is inversely proportional to $\Delta\theta$ and directly proportional to Δd. f is a PI controller. If the distance between two robots Δd is less than a certain value, the later robot moves backward. When the later robot moves into the infrared range, the infrared-based subroutine is called.
- Infrared-based docking controller. In the near range, k_d is scaled up to control v to minimize the distance and k_θ is adjusted to control ω until the infrared signal reaches a threshold. f is a PI controller.

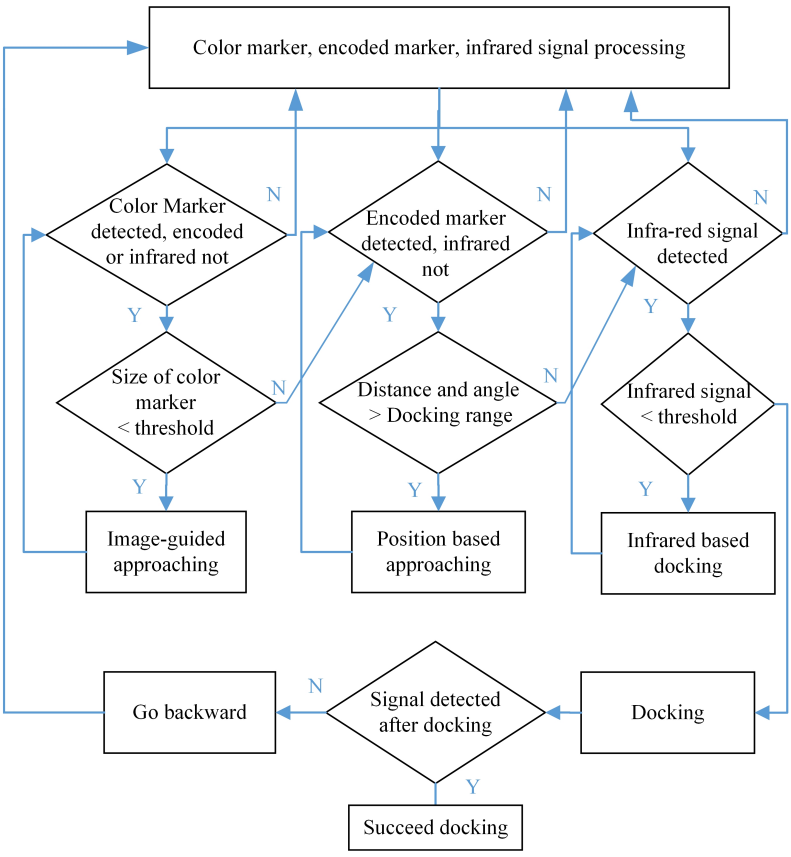

Figure 10. Control flowchart and switching scheme between different states.

Once the corresponding sensor detects nothing in three subroutines, it will move backward to search for the markers and infrared signal. After docking, the CAN bus is connected and a confirmation frame is communicated.

3.4. Obstacle Crossing Method

If there are obstacles in the environments, the robots can maneuver to avoid them, but in some cases such as wide obstacles, they only can cross them, which is the process

described in this paper. The assembled entity has a tree-like topology and a series of orthogonal joints. When the robots encounter an obstacle of a certain height, they can lift themselves and cross it using mobile chassis and joints. As for a snake-like structure, they use chained caterpillar tracks to move on flat ground. Before reaching the obstacle, the first module is lifted above the obstacle and all the modules move forward until the second module approaches the obstacle. Next, the second module is lifted and all the modules move forward until the third module approaches the obstacle and if the modules already lifted over the obstacle have passed beyond the obstacle, the later module's joint rotates inversely to lay the passed module onto the ground vertically. According to this process, all the modules cross in sequence.

In another case, when one SMMRob encounters a gap, it will call other modules to dock and assemble into a chained entity. They can move over the gap and release the front module and the rest move backward. In addition, the connected modules can pass the rough terrain and climb a stair by keeping available contacts on the terrain and enhancing driving. The gait of the other structures of multiple branches need to be well designed, and system experiments using only the snake-like configuration were verified in this study.

4. Experiments and Discussion

4.1. Module Experiments

To evaluate the performance of the robot module, preliminary experiments were performed. The robots were programmed to move and actuate in different cases and geometric and force-measurement tools were used to obtain the parameter values. The weight of an SMMRob module is about 900 g. After testing on flat ground, the maximum transnational speed of the module was 40 cm/s and the maximum payload was 8 kg. Its battery life is 120 min when it moved (other cases depend on joint actuators and computing costs). A variety of terrains were selected to test the terrain trafficability of a single robot, which showed that it could move on a tiled floor, asphalt road, cobbled road, and turf, as shown in Figure 11. It could move up a slope of 28.5° and climb over an 18 mm high obstacle. A video of all the testing experiments is provided in the Supplementary Materials.

Figure 11. Trafficability of a single SMMRob on a variety of terrains and slopes.

As shown in Figure 12, the yaw angle of the joint is ±30° and the pitch angle of the joint is ±45°. It can lift two modules in serial with an actuation torque of 2.7 Nm. The mechanical tolerance of docking is ±8 mm in the lateral direction, ±2 mm in the longitudinal direction, and ±5.7° in deflection. The maximum distance for color marker recognition is 200 cm and the update rate is 30 Hz. The maximum distance of Apriltag recognition is 50 cm in high

resolution (640 × 480 pixels) and 10 cm in lower resolution (160 × 120 pixels). Wireless networking including WiFi and Zigbee can provide communication within a range of about 10–20 m indoors and further outdoors. The main board can be accessed remotely using a router. In a head module, the stereo video can be obtained in real time using WiFi transmission. In Figure 13, video can be captured when SMMRobs move from far away to near the wall. The parameters are summarized in Table 1.

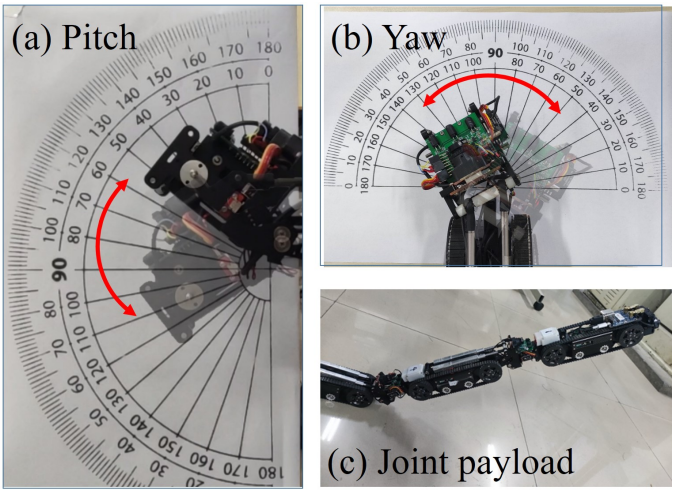

Figure 12. Pitch and yaw angles of the joint and maximum payload.

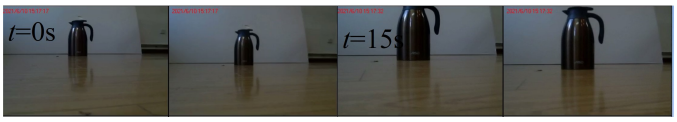

Figure 13. Video screen in the master computer from the stereo camera of the head module.

4.2. Self-Assembling Experiments

Using the controller, docking experiments at different distances and angles were performed. The front robot was placed in situ and the docking robot was laid behind it. As shown in Figure 14, it can be observed that the robot docked with the front one successfully and the path of the moving SMMRob is depicted in a red curve. The lateral distance, longitudinal displacement, and heading angle are depicted in Figure 15. At far, middle, and near distances within certain angles, 70 points were selected as starting locations for test docking. The success or failure cases are presented in Figure 16. A close distance and a small angle proved to be easy for docking, whereas a small distance and large angle was difficult because there not enough travel distance to adjust lateral displacement and heading. According to the data, within a distance of 30 cm and angle of 20°, the success rate was about 50%.

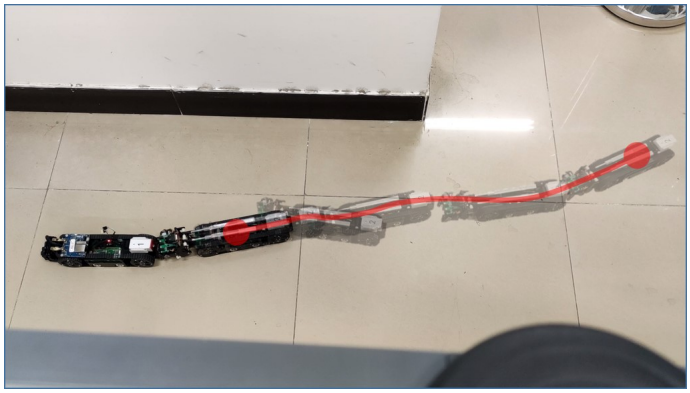

Figure 14. SMMRob docking experiments and the path of the moving robot.

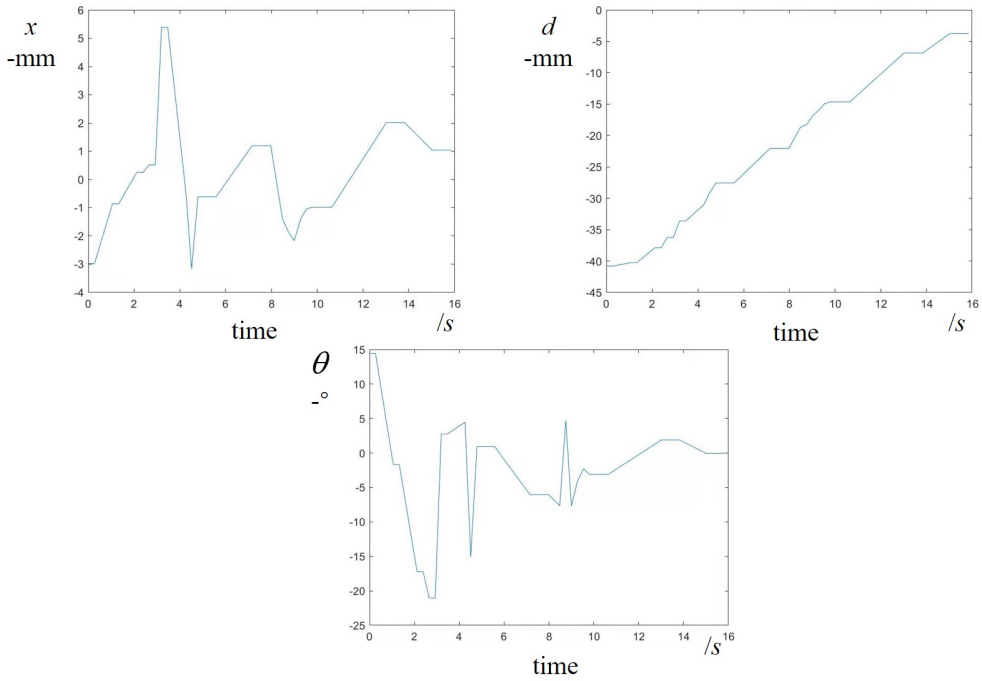

Figure 15. Visual feedback output of a moving SMMRob docking with the front one, depicting the lateral distance, longitudinal displacement, and heading angle.

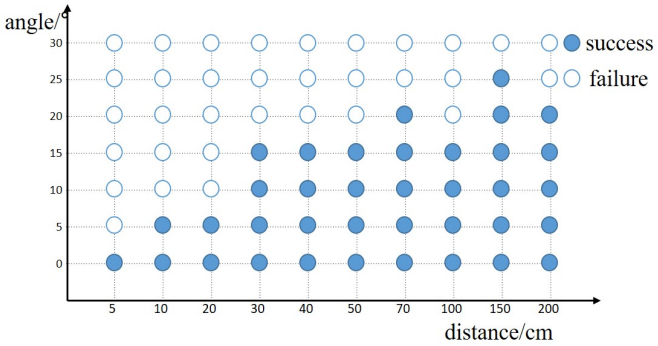

Figure 16. Success and failure results of docking experiments in different ranges.

Five SMMRobs were made to perform self-assembling experiments to build a snake-like composite entity. An SMMRob head module with a lidar and a stereo sensor was placed in situ. Four motion modules docked with the front one according to a self-assembly

sequence and then the assembled entity was able to move in a chain as a whole. As shown in Figure 17, the time required for self-assembly was 155 s, which was single-test data. The time of docking of each robot was different according to its initial position and heading. To form a quadruped structure, a head module with four passive docking panels was placed in situ, four motion modules docked with the head, and then the quadruped was able to lift the four legs to stand, as shown in Figure 18.

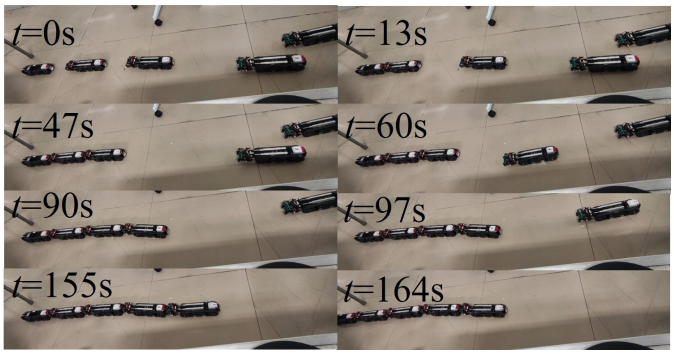

Figure 17. Experiments on the self-assembly of a snake-like composite entity consisting of one SMMRob head module and four body modules and collective motion in a chain.

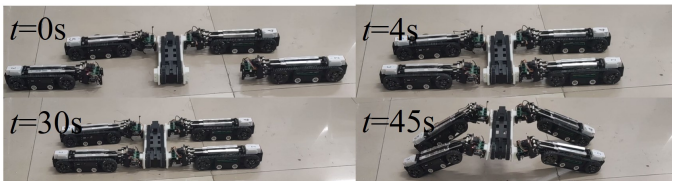

Figure 18. Experiments on the self-assembly of a quadruped structure.

4.3. Systematic Experiments

After self-assembly, the composite entity had a better capacity to respond to the environments. Five SMMRobs formed a snake-like robot and combined caterpillar tracks that were invented by humans and joints that mimicked animals to lift itself to cross a 10 cm high obstacle that was higher than the module, as shown in Figure 19. The time of crossing was 161 s. To avoid rolling, the joint target positions in control periods were interpolated.

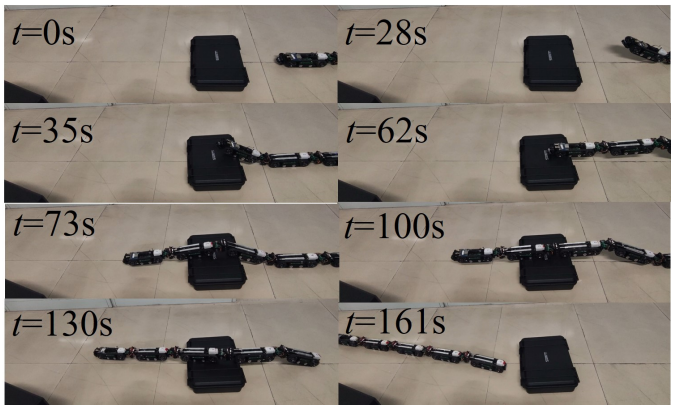

Figure 19. A snake-like robot using combined caterpillar tracks that were invented by humans and joints that mimicked animals to lift itself to cross a tall obstacle.

As shown in Figure 20, the head module was blocked by a gap, detected by the camera and lidar. It called two other modules to connect, and they moved over the gap in a chained train. After that, the head continued moving in the next environment and others moved backward.

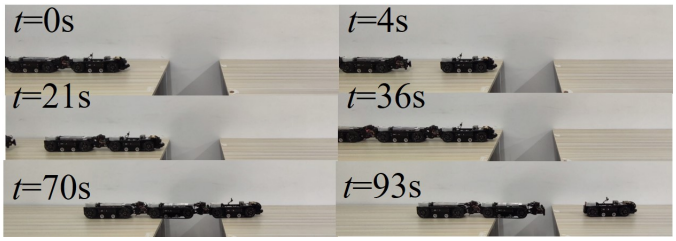

Figure 20. One sensor module, docking with two motion modules in the process of self-assembly, pass over a gap.

An experiment in which a composite entity consisting five modules climbed up a stair was performed. The maximum angle of inclination was 20°, as shown in Figure 21. Because of height limit of the track's beam, it was difficult for the composite entity to climb up steeper stairs.

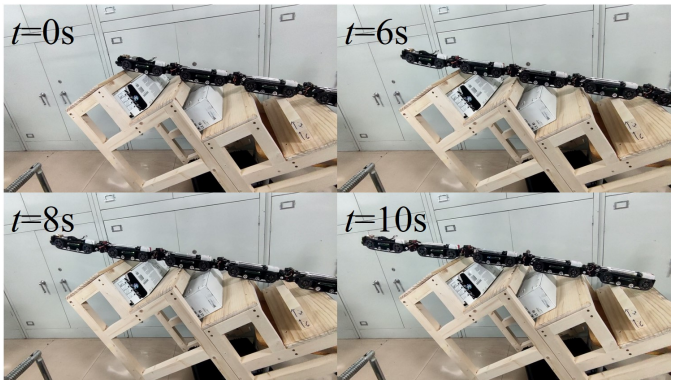

Figure 21. The entity assembled of five modules climbing up a stair with a 20° angle of inclination.

In these experiments, it was found that in order for the assembled structure to conform well to irregular surfaces, it is necessary for the SMMRob modules to actively actuate the joints to match the surface. In this regard, a more complicated motion for a tree-like topology has to be designed and more advanced actuators such as compliant mechanisms need to be considered. In robot docking and connected structures, friction and dynamics are neglected because the robots move at low speed, but when dealing with high-speed docking, friction and dynamics need to be considered further. In addition, when multiple connected robots of multiple branches use tracks to move, skid steering simultaneously could make locomotion difficult and the kinematics of the connected structure has to be designed in this regard.

5. Conclusions

Herein, we present SMMRob, a mobile modular robot that is able to self-assemble. A docking mechanism based on jaws and joint actuation using a 2-SPS parallel mechanism was designed to enhance mechanical interconnections and operation with multiple DoFs. Using three stages of sensors and algorithms, relative positioning and docking controllers have been proposed to guide the docking process. The assembled composite entity can assume a tree-like configuration, such as a linear and quadruped structure. In this paper, a snake-like structure was demonstrated to move in a chained train with active joints. In contrast with the traditional revolute actuators used for the joints of modular robots, the parallel mechanism can make the snake-like body and quadruped's legs thinner, resulting in long links for articular structures. The performance of single modules was tested and a number of docking experiments were performed to evaluate the success rates. Onboard visual perception enhanced the sensing distance and provided information without the use

of a global camera. Self-assembling experiments were evaluated, and the entity was found to be able to traverse obstacles and gaps and climb up a stair.

In the future, the docking algorithm will be further improved to attain a higher success rate. Visual target tracking and a visual inertial odometer could be used to increase positioning precision and stability. We will aim to achieve other configurations such as multi-legged robots. Global and local planning of self-assembling swarm modular robot systems, autonomously responding to environment cues and tasks in real applications, will also be studied.

Supplementary Materials: The following supporting information can be downloaded at: https://www.mdpi.com/article/10.3390/app12063050/s1, Video S1: SMMRob module and self-assembly experiments.

Author Contributions: Conceptualization, H.L.; methodology, H.L., J.L. and J.X.; software, H.W. and H.L.; validation, H.L., H.W., L.C. and Q.W.; investigation, H.W. and L.C.; writing—original draft preparation, H.L.; writing—review and editing, H.L., H.W., L.C., J.L., Q.W. and J.X.; visualization, H.L. and L.C.; supervision, H.L.; project administration, H.L.; funding acquisition, H.L. All authors have read and agreed to the published version of the manuscript.

Funding: This research was funded by the National Key Research and Development Program of China (Grant No. 2018YFB1304602) and National Natural Science Foundation of China (Grant No. 62003048).

Institutional Review Board Statement: Not applicable.

Informed Consent Statement: Not applicable.

Data Availability Statement: Not applicable.

Acknowledgments: Thanks go to X Lab for their assistance with robot design and discussion.

Conflicts of Interest: The authors declare no conflict of interest.

References

1. Petersen, K.H.; Napp, N.; Stuart-Smith, R.; Rus, D.; Kovac, M. A review of collective robotic construction. *Sci. Robot.* **2019**, *4*, eaau8479. [CrossRef] [PubMed]
2. Reid, C.R.; Lutz, M.J.; Powell, S.; Kao, A.B.; Couzin, I.D.; Garnier, S. Army ants dynamically adjust living bridges in response to a costbenefit trade-off. *Proc. Natl. Acad. Sci. USA* **2015**, *112*, 15113–15118. [CrossRef] [PubMed]
3. Yim, M.; Shen, W.M.; Salemi, B.; Rus, D.; Moll, M.; Lipson, H.; Klavins, E.; Chirikjian, G.S. Modular self-reconfigurable robot systems [Grand challenges of robotics]. *IEEE Robot. Autom. Mag.* **2007**, *14*, 43–52. [CrossRef]
4. Chirikjian, G. Kinematics of a metamorphic robotic system. In Proceedings of the 1994 IEEE International Conference on Robotics and Automation, San Diego, CA, USA, 8–13 May 1994; IEEE Computer Society Press: Washington, DC, USA, 1994; Volume 2, pp. 449–455. [CrossRef]
5. Kirby, B.T.; Aksak, B.; Campbell, J.D.; Hoburg, J.F.; Mowry, T.C.; Pillai, P.; Goldstein, S.C. A modular robotic system using magnetic force effectors. In Proceedings of the IEEE International Conference on Intelligent Robots and Systems, San Diego, CA, USA, 29 October–2 November 2007; pp. 2787–2793. [CrossRef]
6. Hauser, S.; Mutlu, M.; Ijspeert, A.J. Kubits: Solid-State Self-Reconfiguration with Programmable Magnets. *IEEE Robot. Autom. Lett.* **2020**, *5*, 6443–6450. [CrossRef]
7. Romanishin, J.W.; Mamish, J.; Rus, D. Decentralized Control for 3D M-Blocks for Path Following, Line Formation, and Light Gradient Aggregation. In Proceedings of the 2019 IEEE/RSJ International Conference on Intelligent Robots and Systems (IROS), Macau, China, 3–8 November 2019; pp. 4862–4868. [CrossRef]
8. Sastra, J.; Chitta, S.; Yim, M. Dynamic rolling for a modular loop robot. *Int. J. Rob. Res.* **2009**, *28*, 758–773. [CrossRef]
9. Sproewitz, A.; Moeckel, R.; Maye, J.; Ijspeert, A.J. Learning to move in modular robots using central pattern generators and online optimization. *Int. J. Rob. Res.* **2008**, *27*, 423–443. [CrossRef]
10. Murata, S.; Kakomura, K.; Kurokawa, H. Toward a scalable modular robotic system. *IEEE Robot. Autom. Mag.* **2007**, *14*, 56–63. [CrossRef]
11. Hauser, S.; Mutlu, M.; Léziart, P.A.; Khodr, H.; Bernardino, A.; Ijspeert, A.J. Roombots extended: Challenges in the next generation of self-reconfigurable modular robots and their application in adaptive and assistive furniture. *Rob. Auton. Syst.* **2020**, *127*, 103467. [CrossRef]
12. O'Grady, R.; Groß, R.; Christensen, A.L.; Dorigo, M. Self-assembly strategies in a group of autonomous mobile robots. *Auton. Robots* **2010**, *28*, 439–455. [CrossRef]

13. Dorigo, M.; Floreano, D.; Gambardella, E.A. Swarmanoid: A novel concept for the study of heterogeneous robotic swarms. *IEEE Robot. Autom. Mag.* **2013**, *20*, 60–71. [CrossRef]
14. Liu, W.; Winfield, A.F. Autonomous morphogenesis in self-assembling robots using IR-based sensing and local communications. In *International Conference on Swarm Intelligence*; Lecture Notes in Computer Science (Including Its Subseries Lecture Notes in Artificial Intelligence (LNAI) and Lecture Notes in Bioinformatics (LNBI)); Springer: Berlin/Heidelberg, Germany, 2010; Volume 6234 LNCS, pp. 107–118. [CrossRef]
15. Wolfe, K.C.; Moses, M.S.; Kutzer, M.D.; Chirikjian, G.S. M^3Express: A low-cost independently-mobile reconfigurable modular robot. In Proceedings of the IEEE International Conference on Robotics and Automation, Saint Paul, MN, USA, 14–18 May 2012; pp. 2704–2710. [CrossRef]
16. Davis, J.D.; Sevimli, Y.; Eldridge, B.R.; Chirikjian, G.S. Module design and functionally non-isomorphic configurations of the Hex-DMR II system. *J. Mech. Robot.* **2016**, *8*, 1–11. [CrossRef]
17. Rubenstein, M.; Cornejo, A.; Nagpal, R. Programmable self-assembly in a thousand-robot swarm. *Science* **2014**, *345*, 795–799. [CrossRef] [PubMed]
18. Zhakypov, Z.; Mori, K.; Hosoda, K.; Paik, J. Designing minimal and scalable insect-inspired multi-locomotion millirobots. *Nature* **2019**, *571*, 381–386. [CrossRef]
19. Li, S.; Batra, R.; Brown, D.; Chang, H.D.; Ranganathan, N.; Hoberman, C.; Rus, D.; Lipson, H. Particle robotics based on statistical mechanics of loosely coupled components. *Nature* **2019**, *567*, 361–365. [CrossRef]
20. Ozkan-Aydin, Y.; Goldman, D.I. Self-reconfigurable multilegged robot swarms collectively accomplish challenging terradynamic tasks. *Sci. Robot.* **2021**, *6*, eabf1628. [CrossRef] [PubMed]
21. Daudelin, J.; Jing, G.; Tosun, T.; Yim, M.; Kress-Gazit, H.; Campbell, M. An integrated system for perception-driven autonomy with modular robots. *Sci. Robot.* **2018**, *3*, eaat4983. [CrossRef]
22. Fu, Q.; Li, C. Robotic modelling of snake traversing large, smooth obstacles reveals stability benefits of body compliance. *R. Soc. Open Sci.* **2020**, *7*, 191192. [CrossRef] [PubMed]
23. Paulos, J.; Eckenstein, N.; Tosun, T.; Seo, J.; Davey, J.; Greco, J.; Kumar, V.; Yim, M. Automated Self-Assembly of Large Maritime Structures by a Team of Robotic Boats. *IEEE Trans. Autom. Sci. Eng.* **2015**, *12*, 958–968. [CrossRef]
24. Mateos, L.A.; Wang, W.; Gheneti, B.; Duarte, F.; Ratti, C.; Rus, D. Autonomous latching system for robotic boats. In Proceedings of the IEEE International Conference on Robotics and Automation (ICRA), Montreal, QC, Canada, 20–24 May 2019; Volume 2019-May, pp. 7933–7939. [CrossRef]
25. Litman, Y.; Gandhi, N.; Phan, L.T.X.; Saldana, D. Vision-Based Self-Assembly for Modular Multirotor Structures. *IEEE Robot. Autom. Lett.* **2021**, *6*, 2202–2208. [CrossRef]
26. Oung, R.; D'Andrea, R. The Distributed Flight Array: Design, implementation, and analysis of a modular vertical take-off and landing vehicle. *Int. J. Rob. Res.* **2014**, *33*, 375–400. [CrossRef]
27. Wei, H.; Chen, Y.; Tan, J.; Wang, T. Sambot: A self-assembly modular robot system. *IEEE/ASME Trans. Mechatron.* **2011**, *16*, 745–757. [CrossRef]
28. Li, H.; Wang, T.; Wei, H.; Meng, C. Response Strategy to Environmental Cues for Modular Robots with Self-Assembly from Swarm to Articulated Robots. *J. Intell. Robot. Syst. Theory Appl.* **2016**, *81*, 359–376. [CrossRef]
29. Li, H.; Wang, T.; Chirikjian, G.S. Self-assembly planning of a shape by regular modular robots. In *Advances in Reconfigurable Mechanisms and Robots II*; Mechanisms and Machine Science; Springer: Berlin/Heidelberg, Germany, 2016; Volume 36, pp. 867–877. [CrossRef]